Journal of Biomechanics 47 (2014) 2826–2830

Contents lists available at ScienceDirect

Journal of Biomechanics

journal homepage: www.elsevier.com/locate/jbiomech
www.JBiomech.com

Short communication

Effects of fluid structure interaction in a three dimensional model of the spinal subarachnoid space

Shaokoon Cheng [a,b,*], David Fletcher [c], Sarah Hemley [d], Marcus Stoodley [d], Lynne Bilston [b]

[a] Department of Engineering, Macquarie University, Australia
[b] Neuroscience Research Australia, Australia
[c] School of Chemical of Biomolecular Engineering, University of Sydney, Australia
[d] Australian School of Advanced Medicine, Macquarie University, Australia

ARTICLE INFO

Article history:
Accepted 17 April 2014

Keywords:
Spinal cord
Cerebrospinal fluid dynamics
Syringomyelia

ABSTRACT

It is unknown whether spinal cord motion has a significant effect on cerebrospinal fluid (CSF) pressure and therefore the importance of including fluid structure interaction (FSI) in computational fluid dynamics models (CFD) of the spinal subarachnoid space (SAS) is unclear. This study aims to determine the effects of FSI on CSF pressure and spinal cord motion in a normal and in a stenosis model of the SAS. A three-dimensional patient specific model of the SAS and spinal cord were constructed from MR anatomical images and CSF flow rate measurements obtained from a healthy human being. The area of SAS at spinal level T4 was constricted by 20% to represent the stenosis model. FSI simulations in both models were performed by running ANSYS CFX and ANSYS Mechanical in tandem. Results from this study show that the effect of FSI on CSF pressure is only about 1% in both the normal and stenosis models and therefore show that FSI has a negligible effect on CSF pressure.

1. Introduction

As CSF flow is pulsatile and the spinal cord is not held rigidly within the human spinal canal, the spinal cord moves within the spinal canal during the cardiac cycle. This motion may change if there is obstruction to CSF flow in the spinal subarachnoid space, and spinal cord motion has been observed to increase in spinal cord injured patients (e.g. McCullough et al., 1990). However, CFD models of the spinal subarachnoid space have rarely included the dynamic fluid-structure interaction (FSI) between the CSF and the tissues of the central nervous system.

In one of the few studies to determine the effects of fluid structure flow interaction in the central nervous system, Fin and Grebe (2003) showed that there is a 5% difference in CSF pressure in the cerebral aqueduct when the interaction between CSF flow and the surrounding soft tissues were included in a model. While FSI has been modelled in two dimensional models of CSF flow in the SAS (e.g. Bertram et al., 2008), to the best of our knowledge, how CSF dynamics, and in particular CSF pressure, are affected by the interaction between CSF and the spinal cord have not been demonstrated in a three-dimensional anatomically accurate model. The magnitude of any bias introduced by neglecting this effect is important to understand, and will inform future models of the CSF and central nervous system dynamics.

In this study, we aim to determine the effects of FSI between CSF and the spinal cord on CSF pressure and spinal cord motion in a normal and stenosis model of the spinal subarachnoid space. We hypothesise that the effect of FSI is negligible in both the normal and stenosis models.

2. Methods

Axial anatomical images and cardiac gated phase-contrast flow measurements of the spinal SAS were acquired from a healthy subject (22 year old female; 52 kg) using a 3-T MRI scanner (Achieva 3TX, Philips Medical Systems, Best, The Netherlands) using standard clinical protocols. CSF flow measurements were obtained at the base of skull (BOS) and T2 spinal level. Imaging parameters for a typical CSF flow measurement were repetition time, 21 ms; echo time, 7.3 ms; temporal phases, 19; flip angle, 10°; field of view, $200 \times 200\ mm^2$ and slice thickness, 5 mm. The MRI data were from a control subject in a larger study examining CSF flow in syringomyelia. This study was approved by the Human Research Ethics Committee of the University of New South Wales, Australia and informed written consent was obtained. The study was conducted according to the Declaration of Helsinki.

* Corresponding author at: Department of Engineering, Macquarie University, Sydney, NSW 2109, Australia.
E-mail address: shaokoon.cheng@mq.edu.au (S. Cheng).

http://dx.doi.org/10.1016/j.jbiomech.2014.04.027
0021-9290/

2.1. Geometry reconstruction

Separate 3D models of the spinal SAS and spinal cord were constructed using the MR anatomical images. The method used to construct the models is similar to that described in Cheng et al. (2012) and Clarke et al. (2013). Briefly, this was achieved by first manually outlining the boundaries of the spinal subarachnoid space and spinal cord on the axial images. The contours were then compiled to build a volumetric spline representation (Surfdriver, version 3.5). These splines were exported to Rhinoceros (V3, McNeel, Seattle, USA) where the surfaces of the spinal SAS and spinal cord for the normal model were reconstructed. The stenosis model was derived from the normal model by reducing the volume of the SAS by 20% smoothly over the T4 level. Four models were simulated: a normal model with and without FSI, and a stenosis model with and without FSI.

2.2. Cerebrospinal fluid modelling

Computational fluid dynamics software ANSYS-CFX (v14, ANSYS Inc., Canonsburg, USA) was used to solve the Navier–Stokes equations in the spinal SAS. The code uses a finite volume approach to solve these equations with bounded second order differencing used in both space and time. The models were meshed with unstructured tetrahedral elements with inflation at the walls (Fig. 1). The meshing controls used in our previous studies were adapted to give a mesh that resolved the flow well (Cheng et al., 2012). CSF was modelled as an incompressible, Newtonian fluid with a dynamic viscosity of 1 mPa s (Bloomfield et al., 1998). The CSF flow velocity measured at the base of skull in the imaging study was fitted with a Fourier series and assigned as the input CSF flow velocity at the rostral end of the model. The reference ('gauge') pressure (0 Pa) was set at the caudal boundary (outlet). The dura at the outer edge of the spinal subarachnoid space was assumed to be rigid. The solution was run as a transient with the prescribed time-varying inlet flow and quasi-steady-state was achieved at the second cardiac cycle. CSF flow was assumed to be laminar, and this was confirmed by checking the Reynolds number throughout the flow domain ($Re < 100$). The mesh size and time step were selected based on our previous work that has shown these values provide mesh and time step independent results. FSI simulations typically took 5 h to run on a modern quad core processor.

2.3. Spinal cord modelling

The deformation and displacement of the spinal cord were calculated using the ANSYS Structural solver (v14, ANSYS Inc., Canonsburg, USA). This code uses a finite element method and a preconditioned conjugate gradient solver to determine the displacement for a specified force. The spinal cord was meshed with a hexahedral mesh, generated by sweeping a quad mesh on one end face through the length of the model. Mechanical properties of the spinal cord were derived from the low strain 'toe region' of uniaxial mechanical properties of the human spinal cord (with overlying pia mater) (Bilston and Thibault, 1996), resulting in a Young's modulus of 700 kPa. The mechanical properties of the spinal cord are summarised in Table 1. The spinal cord was constrained at the rostral end of the model and displacement normal to the boundary was allowed at the caudal boundary. The structural model had 8100 degrees of freedom.

The fluid structure interaction was modelled by running ANSYS CFX and ANSYS Mechanical in tandem in ANSYS Workbench. At a new time step ANSYS Mechanical is called first and provides the displacement of the spinal cord to the CFD code. The mesh used in the CFD simulation is displaced at the boundary with the spinal cord and smoothed to maintain mesh quality. The CFD code is then run to provide the force on the spinal cord, which is transferred to ANSYS Mechanical, completing a single coupling iteration. At a given time step the flow solution must be stabilised to prevent overshoot and divergence, by setting a source coefficient in the pressure equation at the wall adjacent to the spinal cord to effectively under-relax the effect of the wall motion. The magnitude of this coefficient must be chosen such that the wall displacement approaches its converged value monotonically. This was monitored by plotting the force and displacements within a time step and making sure the behaviour was critically damped, with the damping coefficient being modified as needed. It was necessary to make this damping coefficient dependent on the inlet velocity to ensure the amount of damping was correct at all stages of the simulation. Typically 40 coupling iterations were employed at each time step to ensure proper convergence of the coupled system. A time step of 0.01 s was used, being a compromise between being too large and missing details of the flow and too small, which makes such coupled equations unstable because of the large accelerations caused by small displacements.

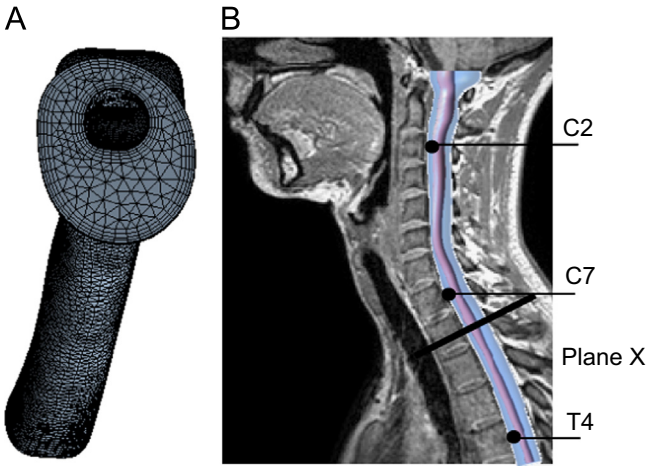

Fig. 1. (A) Mesh model (top view) of the SAS with inflation at the walls. (B) Computational model superimposed on MRI image of subject. The figure also shows the anatomical locations of monitoring points in the anterior SAS at C2, C7 and T4. Plane X is a plane perpendicular to the spine at T1.

Table 1
Mechanical properties of the spinal cord used in the computational models.

	Values	Reference
Young's modulus	700 kPa	Bilston and Thibault (1996)
Density	1050 kg m^{-3}	Cheng et al. (2010)
Poisson's ratio	0.45	Cheng and Bilston (2007)

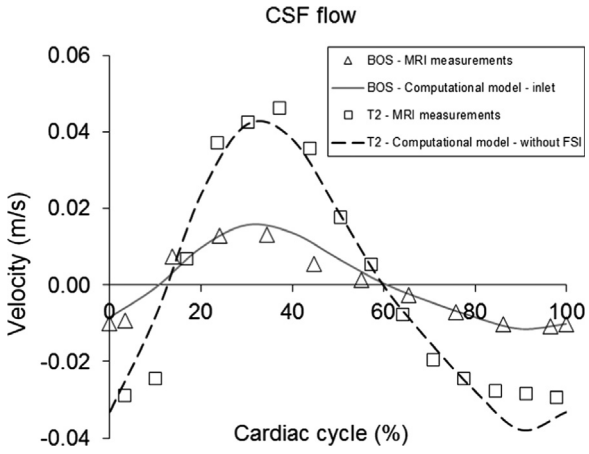

Fig. 2. Phase-contrast MRI measurements and CSF velocity in normal model (without FSI). BOS – Base of skull, T2 – second thoracic vertebra.

3. Results

Fig. 2 shows the MRI measurements (symbols) and matching CSF flow velocity in the rigid model (lines) at the BOS and T2. Fig. 3 shows the CSF pressure anterior to the spinal cord at three different spinal levels (see Fig. 1B for locations of points monitored) in the normal and stenosis models. The maximum pressure difference between the models with and without FSI in both cases is only ~1% and this is at C2 and at 18% of the cardiac cycle.

Fig. 4A shows the motion of the spinal cord in the normal and stenosis models at C2, C7 and T4. Spinal cord motion is primarily in the antero-posterior direction with minimal lateral motion. Spinal cord motion is in the ventral direction from 17% to 65% of the cardiac cycle and in the dorsal direction for other phases of the cardiac cycle. Spinal cord motion is the highest at C7 and this occurs at 40% of the cardiac cycle in both models. Spinal cord motion is larger in the stenosis model compared to the normal